First principle study of core/shell structure quantum dots

Jingbo Li and Lin-Wang Wang*
Computational Research Division, Lawrence Berkeley National Laboratory, Berkeley, CA 94720
(Dated: February 26, 2004)

The electronic states of core/shell CdSe/CdS and CdSe/CdTe heterostructure quantum dots are studied by large-scale first-principles calculations. According to their natural band-offset alignments CdSe/CdS is a type-I heterostructure and CdSe/CdTe is a type-II heterostructure. We found that, the electron state changes very litte, but the hole wavefunction in CdSe/CdS quantum dots has been localized within the core, while the hole wavefunction in CdSe/CdTe quantum dots is localized within the shell. The hole state in CdSe/CdTe quantum dots has drastically different characteristics as in CdSe and CdSe/CdS quantum dots. The band alignment, strain effect, and quantum confinment are all important to determine the electronic structures of these systems.

PACS numbers: 73.22.-f, 71.15.Mb, 79.60.Jv

During the last decade, technology advances in colloid chemistry have led to fabrication of high quality size-controlled semiconductor nanocrystal quantum dots (QDs). [1] Of special interest are the wet chemical synthesis of two materials core/shell structure QDs, which extends the rich physics of 2D superlattices [2] into the area of 0D QDs. According to their band alignments, the heterostructures can be classified as type-I (the minimum of conduction band and the maximum of valence band are in the same material) or type-II, showing drastic differences in the electronic structure. In 0D heterostructure QDs, the type-I and type-II systems are also expected to show different properties. But in this case, the band alignment effects are coupled with the strong quantum confinements and strong strain effects. These make these systems physically interesting. They also make highly accurate electronic structure calculations necessary. Recently, a number of experimental groups have reported the fabrication of well controlled core/shell structure QDs, such as CdSe/CdS, [3, 4] CdSe/ZnS, [5] InAs/CdSe, [6] and CdTe/CdSe QDs [7]. Their electronic structures and optical properties are carefully studied, and in some cases [4] improved devices are developed based on these core/shell QDs.

Theoretically, a few approaches have been used to study these systems. These include the effective mass method [8], multi-band $k \cdot p$ method [9] and empirical tight-binding method [10]. But all these methods are highly approximated in nature. It has been shown that the applicabilities of the continuum effective mass and $k \cdot p$ theory to the few monolayer size QDs are questionable [11]. The empirical tight-binding method might suffer from its uncertainty of the fitting parameters and poor transferibility from bulk to QDs. Thus, it is much more desirable to do reliable first principle calculations to these systems. Here, using a recently developed charge patching method, we have carried out first principle local density approximation (LDA) calculations for the 2000 atom QDs. To model an ideal passivation, we have used pseudo-hydrogen atoms (with fractional nuclei charges and numbers of electons) on the surface of the QD. Then, atomistic valence force field (VFF) [12] is used to relax the atomic positions. After the atomic positions are relaxed, the total electronic charge density of a given system is generated by assembling of charge motifs on each atoms. These charge motifs are calculated from small prototype systems with similar atomic environments as in the nanosystem. Then the total electron potential is generated from the charge density and the band edge eigen states are solved using the folded spectrum method [13]. The resulting single particle eigen energies have a typical error of $\sim$20 meV compared to direct LDA calculations, and the eigen energy splittings within valence band and conduction band have typical errors of just $\sim$5 meV. Thus the current calculation has almost the same accuracy as a straight forward direct first principle LDA calculation. The details of this method will be reported elsewhere. We have used planewave basis sets and norm conserving pseudopotentials with a planewave cutoff of 35 Ryd. This results in a real space grid of $384\times360\times360$ to calculate the following systems. Spin-orbit interaction is included in the single particle's Schrodinger equation.

Two core/shell QDs with wurtzite (WZ) crystal structure are studied: CdSe/CdS and CdSe/CdTe. The diameter of the core is 29.03$\mathring{A}$ and the thickness of the shell is 7.6$\mathring{A}$. These core/shell system will be compared with the pure CdSe quantum dot results with a diameter of 44.23$\mathring{A}$. For the VFF parameters, we have used the experimental bulk lattice constants, for CdSe: $a = 4.3\mathring{A}$; CdS: $a = 4.11\mathring{A}$; CdTe: $a = 4.58\mathring{A}$.

There are several questions we like to answer through this study: What is the band alignment of these structures? How does the strain effect changes the band alignment? What are the qualitative difference between the type-I and type-II core/shell structures? Are the shell strong enough to confine or shield the single particale states? What are the effects on the band gap, optical transition matrix elements, and electron-hole Coulomb interactions? We have the following findings.

(1) *Band alignment of CdSe/CdS and CdSe/CdTe het-*

*Electronic address: lwwang@lbl.gov

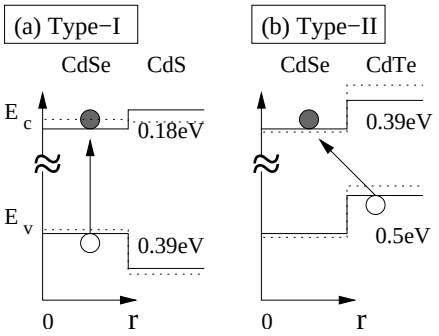

FIG. 1: Schematic plot of the band alignments discussed in this letter. The solid arrows denote the lowest band gap.

erojunctions: We first use self-consistent LDA to calculate the band alignment of CdSe/CdS and CdSe/CdTe via a 2D superlattice. The resulting natural (both materials in their relaxed lattice constants) band offsets including the spin-orbit interaction are shown in Fig. 1. As we can see, the CdSe/CdS has a type-I band alignment, and the CdSe/CdTe has a type-II band alignment.Our calculation is in quantitative agreement with Ref.[14] calculated with an all electron linearized augmented plane wave (LAPW) method. Note that, calculated by LDA, there is a significant error in our band gap. However, since the conduction band alignment in Fig.1 is almost the same as the results with the experimental band gap [14], there is no need to correct the absolute LDA band gap in our study. In some early studies, it is assumed that the CdSe/CdS has a type-II band alignment [15, 16], but that is not consistent with the recent *ab initio* calculations [14] and experiments [3]. In the tight-binding calculation of Ref.[10], a type-II band alignment is used for CdSe/CdS, and a very large 1.3 eV valence band offset (compared to our ab initio results in Fig.1) is used in their fitting. This highlights the advantages of the *ab initio* calculations.

After the VFF relaxation, the QD CdS layer has a tensile strain, while CdTe has a compressive strain. This results in a modified band alignment shown as the dash lines in Fig.1. A major change is the conduction band alignment in the CdSe/CdS QD. After the relaxation, there is almost no electron confinement in this system, while the confinement in CdSe/CdTe increased significantly. Note that, Fig.1 is used to analysis the results, not used to fit any potentials in the following calculations. In our first principle calculation, there is no need for fittings of any kinds.

(2) *Wavefunction distribution :* The contour plots of wavefunction squares on a cross section perpendicular to the WZ c-axis are shown in Fig.2 for pure CdSe, CdSe/CdS, and CdSe/CdTe. First, the singlet conduction band minimum (CBM) states have a s-like symmetry, while the singlet valence band maximum (VBM) states consist mainly of two bulk Bloch states of Γ_9 and Γ_7, which have p_{xy} and p_z characters respectively. Comparing to the pure CdSe case, the CdS and CdTe shell have their main effects on the VBM. The CBM states have only been modified slightly. The small changes of the electron states are attributed to the small effective masses of the conduction band and relatively small band offsets. Notice that, in Ref.[10] the tight-binding calculation produces a dramatic change in the electron state, in sharp contrast with our ab initio results. For CdSe/CdS QD, 96% of the VBM is contained inside the CdSe core. For CdSe/CdTe QD, most of the VBM is within the shell. More strikingly, we see a well defined hexagon for the VBM wavefunction, and the atomic character of the wavefunction is a p_{xy} along the lines of the hexagon. This surprising arrangement of the wavefunction can be understood by the quantum confinment effect. The confinment

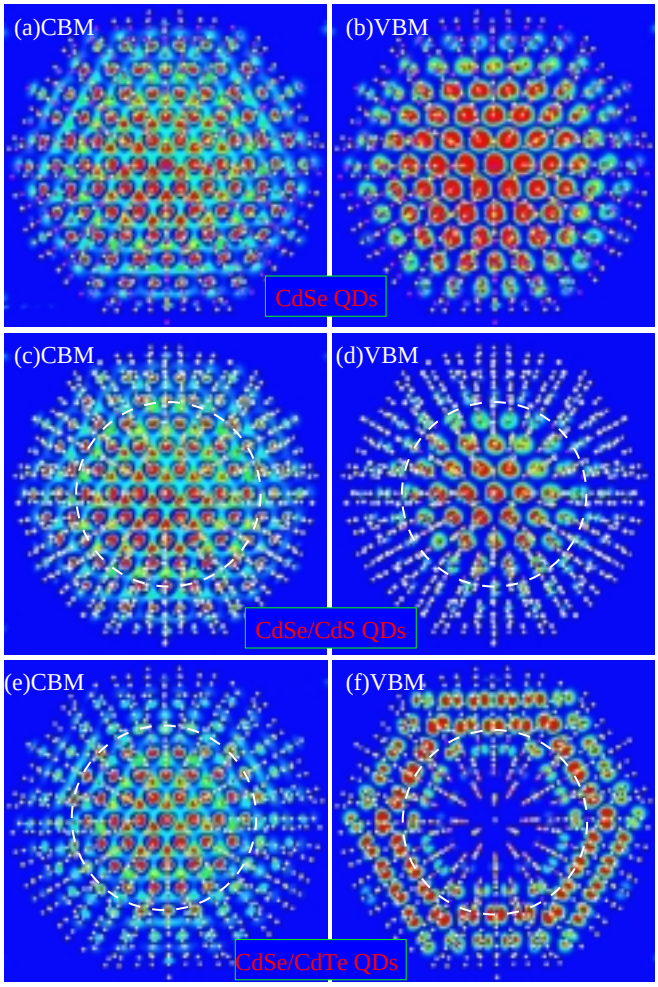

FIG. 2: Contour plot of charge density distribution of CBM and VBM state of (a),(b) CdSe QDs; (C), (d) CdSe/CdS (core/shell) QDs; (e), (f) CdSe/CdTe (core/shell) QDs. Yellow dots represent Cd-atom, magenta dots represent Se-atom, white dots represent S or Te atom. The white dashed-circles indicate the boundaries between different materials. The surface atoms are not ploted in this figure. Red, yellow, green, and blue colors indicate electron density from higher to lower.

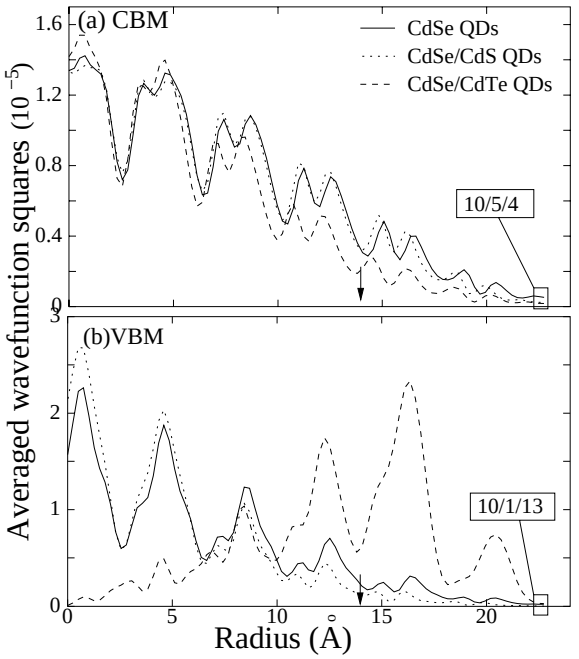

FIG. 3: Averaged wavefunction squares for (a)CBM and (b) VBM states of CdSe QDs, CdSe/CdS QDs, and CdSe/CdTe QDs. The arrows indicate the boundaries of CdSe/CdS or CdSe/CdTe interface.

effect within the shell comes mainly from the radius direction. By aligning the p character along the lines of the hexagon, the VBM will have a heavy hole effective mass in the direction of the confinment. This situation is different from the VBM in spherical confinment as in the case of CdSe and CdSe/CdS QDs.

Fig.3 plots the spherically averaged wavefunction squares at different radius. We see that, for CBM, the situation for CdSe and CdSe/CdS QDs are quite similar in agreement with Fig.1, while for CdSe/CdTe QD there are some significant changes in the electron state. The averaged CBM wavefunction squares at the surface of the QDs have a ratio of 10/5/4 for CdSe, CdSe/CdS and CdSe/CdTe QDs, while this ratio for VBM is 10/1/13. Thus, for the CdSe/CdS QD, the VBM wavefunction is significantly suppressed near the dot surface. This is consistent with the experimental results of the decreased oxidization rate in the CdSe/CdS QD[3]. In order to be oxidized, the hole wavefuntion needs to be leaked out into the surface. This is reduced by about 10 times according to our calculation. For VBM of CdSe/CdTe QD, we see predominant peak inside the shell region. The contrast between the CdSe/CdS and CdSe/CdTe QDs signifies the qualitative differences between the type-I and type-II core/shell QDs.

(3) *Band gap and optical transition intensities:* In our calculation, the three QDs have the same overall size. But their band gaps are very different. The QDs band gap are $E_g = 1.286, 1.393, 0.724eV$ for CdSe, CdSe/CdS, and CdSe/CdTe respectively. This suggests that the shell-layer of the QDs has added another dimention to tailor the band gap of the QDs. The optical transition matrix element between the CBM and VBM states is given by $Q_{xyz} = | < \psi_{CBM}|P_{xyz}|\psi_{VBM} > |^2$. We find $Q = 1.712, 2.071, 0.487 \times 10^{-3}eV$ for the three QDs in Fig.2. From CdSe, CdSe/CdS QD to CdSe/CdTe QD, the character of VBM state has changed drastically, although their symmetry remains the same. The absorption spectra of type-II QDs in Fig. 2 of Ref.[7] show a featureless absorption tail into the red and near-infrared. This is in agreement with our result of very weak optical transition intensity from CBM to VBM state in the CdSe/CdTe QD.

(4) *Strain effect on the heterostrcture QDs:* As we have shown in Fig.1, strain changes the band offset. As a result of that, the strain also changes the band gaps of the QDs. For CdSe/CdS QD, if ideal WZ atomic positions (with average lattice constant) are taken without VFF relaxation, the Eg would be 1.329eV. After the VFF atomic relaxation, the Eg is 1.393eV. So, the strain effect is 64meV. For CdSe/CdTe QD, the atomic relaxation causes a change of 163meV in the band gap. This indicates that in a heterostructure QD, the band alignment, the strain effects and the quantum confinements are all important.

(5) *Electron hole Coulomb interaction:* The strong localizations of wavefunctions shown in Fig. 2 also demonstrate themselve in the screened electron-hole Coulomb interaction, which is definded as $E_b = \int\int \frac{|\psi_e(\mathbf{r_1})^2||\psi_h(\mathbf{r_2})^2|}{\epsilon(\mathbf{r_1}-\mathbf{r_2})|\mathbf{r_1}-\mathbf{r_2}|} d\mathbf{r_1}d\mathbf{r_2}$ where $\epsilon(\mathbf{r_1}-\mathbf{r_2})$ is an nonlocal screening function for a quantum dot.[13] Using the above formula, we obtained $E_b = 0.148, 0.163, 0.103eV$ for CdSe, CdSe/CdS and CdSe/CdTe QDs. The strong hole confinment in CdSe/CdS causes it to have the largest electron-hole Coulomb interaction.

This work was supported by U.S. Department of Energy under Contract No. DE-AC03-76SF00098. This research used the resources of the National Energy Research Scientific Computing Center.

[1] A. P. Alivisatos, Science **271**, 933 (1996).
[2] L. Esaki, IEEE Quant. Electron. **QE-22**, 1611 (1986).
[3] X. Peng, M. C. Schlamp, A. V. Kadavanich, A. P. Alivisatos, J. Am. Chem. Soc.**119**, 7019 (1997).
[4] M. C. Schlamp, X. Peng, A. P. Alivisatos, J. Appl. Phys. **82**, 5837 (1997).
[5] M. A. Hines, P. Guyot-Sionnest, J. Phys. Chem. **100**, 468 (1996).
[6] Y. W. Cao, U. Banin, Angew. Chem. Int. Ed. **38**, 3692 (1999).

[7] S. Kim, B. Fisher, M. Bawendi, J. Am. Chem. Soc. **125**, 11466 (2003).
[8] D. Schooss, A. Mews. A. Eychmuller, H. Weller, Phys. Rev. B **49**, 17072 (1994).
[9] E. P. Pokatilov, V. A. Fonoberov, V. M. Fomin, J. T. Devreese, Phys. Rev. B **64**, 245329 (2001).
[10] S. Pokrant, K. B. Whaley, Eur. Phys. J. D**6**, 255 (1999).
[11] H.X. Fu, L. W. Wang, A. Zunger, Phys. Rev. B **57**, 9971 (1998).
[12] C. Pryor, J. Kim, L. W. Wang, A. J. Williamson, A. Zunger, J. Appl. Phys. **83**, 2548 (1998).
[13] L. W. Wang, A. Zunger, J. Phys. Chem. B **102**, 6449 (1998).
[14] S. H. Wei, S. B. Zhang, A. Zunger, J. Appl. Phys. **87**, 1304 (2000).
[15] M.P. Halsall, J.E. Nicholls, J.J. Davies, B. Cockayne, P.J. Wright, A.G. Cullis, Semicond. Sci. Technol. **3**, 1126, (1988).
[16] W. Langbein, M. Heffereich, M. Gruen, C. Klingshirn, H. Kalt, Appl. Phys. Lett. **65**, 2466 (1994).